Trypsin detection using chitosan based fiber optic interferometric sensor

Aroor, Megha Rani

2016

Aroor, M. R. (2016). Trypsin detection using chitosan based fiber optic interferometric sensor. Master’ s thesis, Nanyang Technological University, Singapore.

https://hdl.handle.net/10356/68505

https://doi.org/10.32657/10356/68505

TRYPSIN DETECTION USING CHITOSAN BASED FIBER OPTIC INTERFEROMETRIC SENSOR

MSc (Biomedical Engineering) Dissertation

School of Chemical and Biomedical Engineering

Nanyang Technological University

Singapore

By

MEGHA RANI AROOR

*****

YEAR 2015

Assoc. Prof CHAN CHI CHIU JULIAN, Supervisor

_____

Supervisor
Chemical and Biomedical Engineering

ABSTRACT

There has been remarkable developments in the field of fiber optic sensing technologies for bio-sensing applications. In this study, a novel fiber optic biosensor has been fabricated for sensing trypsin, a protease that helps in degradation of proteins to peptides. A 2 cm long No core sensor was functionalized with Nickel-Chitosan film. Chitosan, a moisture sensitive polymer acted as the chelating agent or the linker polymer which facilitated the binding of the nickel ions to trypsin. The sensor was immersed in different concentrations of trypsin sample and the spectral responses were recorded. The wavelength dips in the transmission spectrum shifted towards lower wavelengths for different concentrations of trypsin. A sensitivity of -0.09 nm $\mu g^{-1}ml^{-1}$ was observed for concentrations of the trypsin sample ranging from 0-200 $\mu g\ ml^{-1}$.

ACKNOWLEDGEMENTS

"At times, our own light goes out and is rekindled by a spark from another person. Each of us has cause to think with deep gratitude of those who have lit the flame within us."

- *Albert Schweitzer*

I would like to thank the school for giving me this opportunity to participate in the project that helped me gain a lot of knowledge from well qualified mentors during the entire course of this learning journey.

My sincere thanks and heartfelt gratitude to my supervisor, Assoc. Prof Chan Chi Chiu Julian, for his encouragement and undeterred faith in me during trying times and for his continued and unstinting support during the entire course of the project.

I would like to express my gratitude to my mentor, Raghunandhan Ravikumar, for helping me in my project even during his busy schedule. He helped me in understanding the concepts better and his guidance truly helped in managing the experiments more effectively. I express my deepest thanks to my lab mates Jemimal Jeyasuriya and Saranya Navaneetham who were there beside me during my trying times and helped me whenever needed, during the entire course of the project. Finally, I would also like to express my heartfelt thanks to my parents and family who were instrumental in believing in me and providing all the support and encouragement.

TABLE OF CONTENTS

LIST OF FIGURES

LIST OF ABBREVIATIONS

SMF	Single mode fiber
NCF	No core fiber
OSA	Optical Spectrum analyzer
PBS	Phosphate Buffer Saline

1. INTRODUCTION

1.1. Background

With tremendous progress in the field of nanotechnology and healthcare, biosensors have been one of the most interesting fields of research over the past few years. Scientists and researchers have developed biosensors for numerous applications in medicine, biotechnology and biomedical applications. One of the major advances in the field of biosensor research has been the use of cost effective optical fibers to be a part of the sensor technology. Optical fibers are being used as a probe or as sensing elements in clinical, pharmaceutical and medical applications [1].

This project summarizes the fabrication and development of a novel fiber optic biosensor for the detection of trypsin. A concise overview of the basic principles involved in fiber optic interferometry is presented. Emphasis is given to the method of fabrication, functionalization technique, and how fiber optic sensors are used as biosensors for sensing trypsin.

1.2. Objective

The main objective of this project is to describe the process of fabrication and performance of a Ni-Chitosan film functionalized No core fiber optic sensor for sensing a serine protease, trypsin. It includes the following sub topics:-

- Design and fabrication of No Core fiber optic sensor
- The technique used for functionalization of the sensor with Ni-Chitosan film.
- Analysis and evaluation of the sensitivity of the sensor to different concentration of trypsin solutions.

1.3. Overview

This project is organized as follows:

Chapter 1 deals with a brief discussion of fiber optic biosensors, including the basics of fiber optics and interferometers.

Chapter 2 includes the method of fabrication, functionalization technique employed and the procedure behind trypsin detection.

Chapter 3 involves the experimental results of the fiber optic sensor used in trypsin detection

Chapter 4 concludes the project with a brief summary, significance and future prospects of fiber-optic biosensors.

1.4. Literature survey

Fiber optics has been one of the most promising and trending technologies over the last few decades. With advancements in the field of fiber optic technology, optical fibers have been extensively used in diverse applications due of their distinctive characteristics [1]. Because of their unique features such as small size and biocompatibility, fiber optic sensors have been used in sensing biological parameters in microenvironments [1]. They are also resistive to electromagnetic interference.

The light waves travelling through the fiber optic sensors are influenced by external factors like temperature, pressure, stress, strain and so on [2]. The interaction with the measurands (quantity that is to be measured) with optical fibers results in modulation of the parameters of the light waves travelling through the optical fibers. The parameters that are modulated are intensity, phase, wavelength and polarization [2].

Intensity of the transmitted light gets modulated by the influence of external environment. These changes in intensity are measured using intensity modulated fiber optic sensors. They are primarily used in the measurement of pressure, vibration, and changes in displacement in medical and industrial applications [2]. Phase modulated sensors operate based on interference phenomenon. The phase of the light in the sensing fiber is compared with that of the reference fiber [2]. In wavelength modulated sensors, the wavelength of light passing through them is modulated [2]. Polarization modulation in birefringent optical fibers is used for the measurement of current and magnetic field wherein the light waves travel with different phase velocities. By changing the optical length, the phase of the light beam is shifted [2].

Fiber optic sensors can also be classified based on two different mechanisms of sensing, namely, intrinsic and extrinsic fiber optic sensors [2]. In extrinsic sensors, optical fibers are used to transmit light from source to the probe attached to the output end of the fiber. The resultant light signal is detected by the detector. Extrinsic sensors are passive and do not play a part in sensing operation. In intrinsic sensors, the optical fibers act as the active sensing element. The measurand modifies the light propagating through the fiber [2].

1.4.1. Optical fibers –principle of operation

Optical fibers are dielectric waveguides and comprise of a transparent core of a higher refractive index surrounded by a cladding surface which forms the jacket with a lower refractive index compared to the core [3]. Figure 1 shows the cross-section of an optical fiber. Light waves traveling through the fiber are confined within the core by the phenomenon of total internal reflection [3]. This makes the optical fibers behave like waveguides. Optical fibers that support many propagation paths are referred to as multimode fibers and those in which light waves travel through a single path are referred to as single mode fibers.

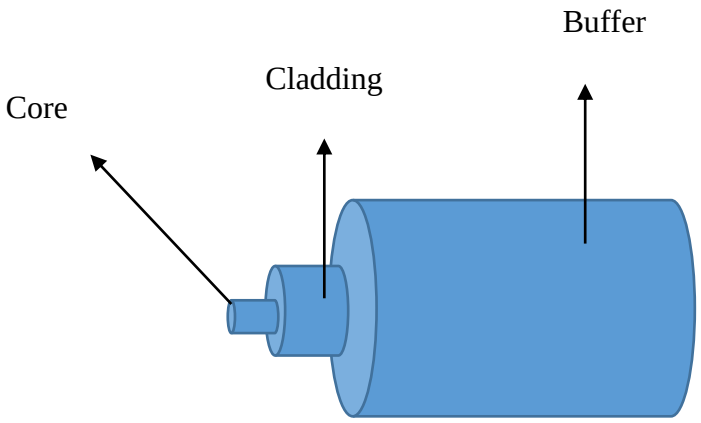

Figure 1: Optical fiber cross section

1.4.1.1. Index of refraction

Index of refraction is a term used to determine the speed of light in a particular medium. It is defined as the ratio of speed of light in vacuum to the speed of light in a particular medium and is given by

$$n = c / v$$

Where c is velocity of light in vacuum and v is velocity of light in the medium. From this equation we can deduce that refractive index of a medium is inversely proportional to the speed of light in that medium. The cladding of the single mode fiber which is made of pure silica has a typical refractive index of 1.444 at 1500nm, and the core made of doped silica is of refractive index value 1.4475 [3].

These refractive indices play are very important role in determining the critical angle. Critical angle is the angle at which total internal reflection occurs. It is denoted by θ_c and is given by the formula

$$\theta c = \sin^{-1}(n_{cladding} / n_{core})$$

Where $n_{cladding}$ is the refractive index of the cladding which is less than the core refractive index, $n_{core.}$

1.4.1.2. Fiber modes

In general, optical fibers support the path of propagation of light waves in two modes, namely single mode and multimode.

1.4.1.2.1. Single- mode

Single mode optical fibers mostly have a core diameter of about 8-10 microns [3]. They support only one mode for the propagation of light waves through the core. Hence, there is no intermodal dispersion in single mode fibers. This serves as an important advantage for using single mode fibers for transmitting light signals over long distances [3].

1.4.1.2.2. Multi-mode

These fibers have an estimate core diameter of 62.5 microns and they support multiple propagation modes for the propagation of light. The waves are guided along the

length of the fiber by the phenomenon of total internal reflection. Rays that are incident at the interface of core and cladding at angles higher than the critical angle get completely reflected [3].

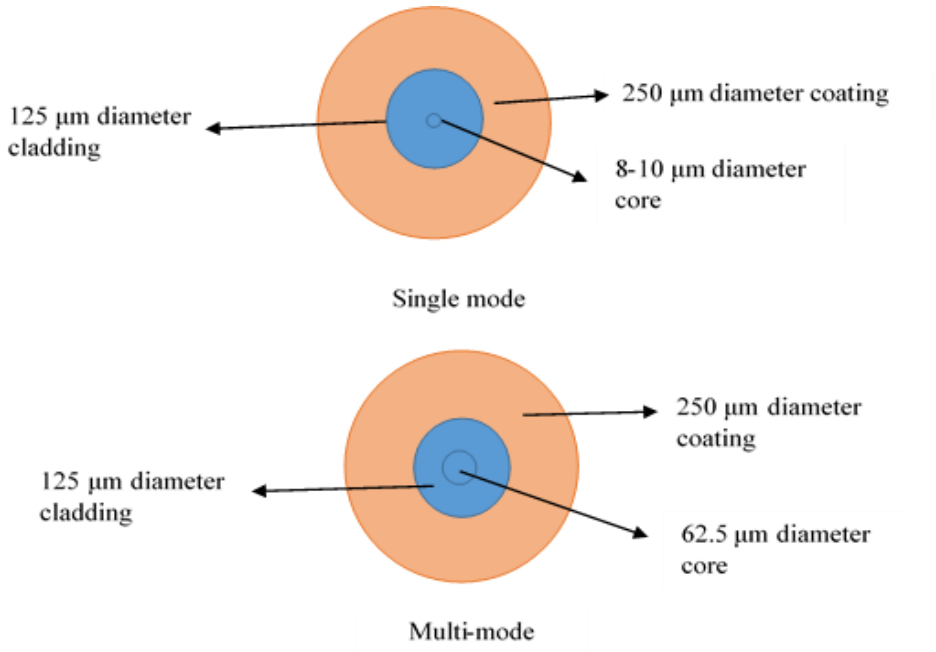

Figure 2: Cross-section of single-mode fiber and multi-mode fiber

Figure 2 shows the cross-section of single and multi-mode fibers.

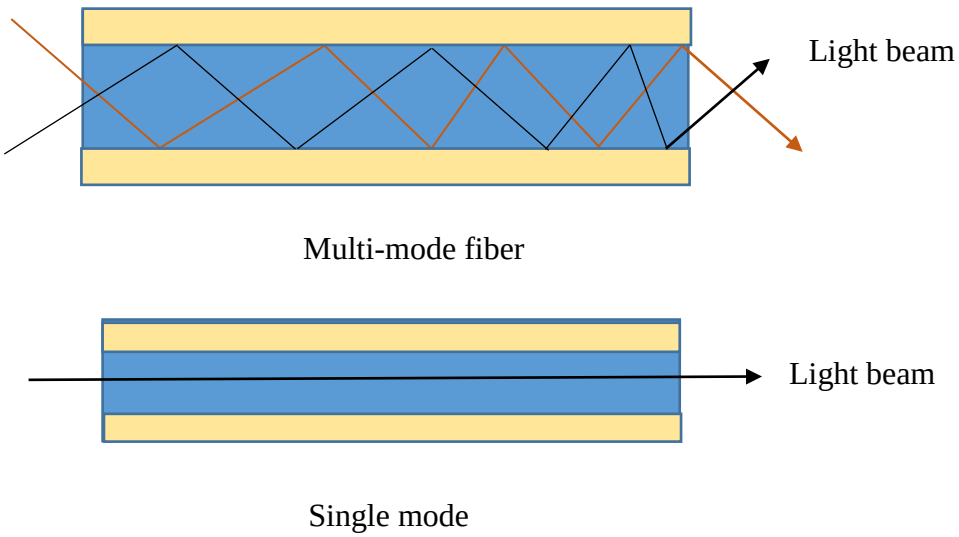

Figure 3: Propagation path of light in single-mode and multi-mode fiber

Figure 3 shows the path of propagation of light in single and multi-mode fibers.

A typical multi-mode fiber fabricated without the cladding layer is termed as a no core fiber. It has a core diameter of 125 microns. The core is made up of undoped silica and is highly sensitive to changes in refractive index. It has been used in a variety of applications such as strain sensing, refractive index sensing and humidity measurement applications [4, 5].

1.4.2. Fiber optic sensor-fabrication

Arc fusion splicing is the common technique used in the fabrication of fiber optic sensors. In this technique, initially the fiber ends are stripped off their polymer coatings and cleaved using a cleaver to make the ends flat using a splicer. The location and the energy of the sparks can be controlled by presetting splicing parameters. A fusion splice loss of less than or equal to 0.05 dB is acceptable [6].

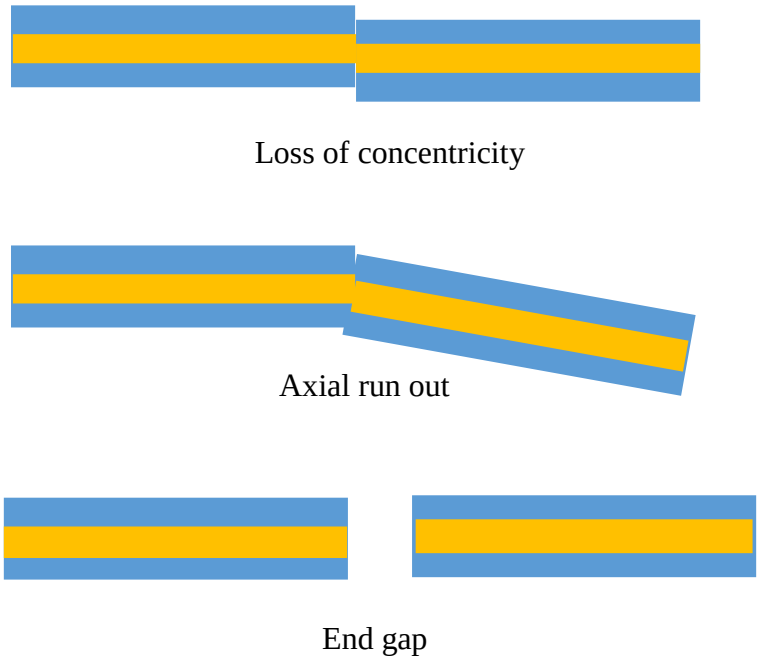

Figure 4: Factors for splice loss

Optical fiber connector/splice loss occurs due to many different factors. The misalignment of the centers of the optical fiber can lead to splice loss. The different

factors that can lead to spice loss is illustrated in Figure 4. Hence, care should to be taken to see that the angle of cut is minimum while cleaving the fibers before splicing them. A large cut angle can result in axial run out which might lead to splice loss. Also, the gap between the optical fibers while splicing also may lead to splice loss. Cleaning of the optical fiber after cleaving is also an essential step to minimize splice loss [6].

1.4.3. Interferometry

Over a few decades, optical fibers have been employed as sensing indices for the measurement of pressure, temperature, pH and change in refractive indices.

Interferometers have been used in the field of science and technology to measure minute changes in displacement, variations in refractive indices and in the measurement of changes in irregularities in surfaces [7]. These instruments have unique characteristics such as dynamic measuring capabilities in three-dimensional motion mapping, analysis and study of resonant frequency structures [8].

1.4.3.1. Basic principles of interferometry

Interferometry is based on a collection of techniques that deals with the superimposition of two waves [7]. When two waves with similar frequencies combine together, it results in an interference pattern determined by the phase difference between the two waves. The interference is constructive if the waves are in phase and destructive if the waves are out of phase [7].

The basic principle behind interferometry is that a beam of light that is coherent in nature is divided into two beams that are identical. The beam splitter is a partially reflecting mirror. The two beams travel in two different paths, and reunite together before approaching the detector.

1.4.3.2. Interferometric techniques

Interferometric techniques are found to be classified based on a number of criteria:

1.4.3.2.1. Homodyne and heterodyne detection

- In homodyne detection, the two beams that undergo interference are of the same wavelength. The intensity change on the detector is measured by the change in phase difference between the two beams. After the two beams reunite, the output intensity is measured and the interference fringe pattern is viewed and recorded.
- In heterodyne detection, either the input signal is shifted to a new frequency range or a weak signal is amplified by using an active mixer. A signal with a comparatively weak input frequency f1 is mixed with a with a strong reference frequency f2 from a local oscillator [7]. The mixing results in the formation of two signals, one with output frequency f1+f2 and the other one with a frequency of f1-f2. These two frequencies are referred to as heterodynes. Typically, for experimental purposes, only one of the equations are used for investigations and hence the unwanted signal is omitted with the help of filters. The output signal intensity is found to be proportional to the product of input signal amplitude [7].

1.4.3.2.2. Double path and common path

- In double path type, the sample and reference beams travel along divergent directions. Michelson and Mach-Zehnder interferometers serve to be good examples. After interacting with the test sample, there is recombination of sample beam with the reference beam thus creating an interference pattern [7].

- In a common path type, both sample and reference beams travel along the same path. Sagnac interferometer is a good example.

1.4.3.2.3. Wavefront splitting and amplitude spitting

- In wavefront splitting, the light wave is divided at a particular point or after emerging from a narrow slit, and recombined after the two waves travel in different paths. Rayleigh interferometer, young's interference experiment, are some of the examples in which we witness wavefront splitting phenomenon [7].
- In amplitude splitting, a partial reflector divides the amplitude of the incident beam into two distinct beams which undergo recombination at a later stage. Michelson, Fabry-Perot, Mach-Zehnder interferometers are some of the examples [7].

1.4.3.3. Types of interferometer configurations

Some of the important ones include Sagnac interferometers, Mach-Zehnder, Michelson and Fabry-Perot interferometer.

1.4.3.3.1. Sagnac interferometers

Sagnac effect is a phenomenon that is induced from rotation. This effect is found to take place in a ring configuration. In this configuration, the source that is used is a single coherent beam or usually an erbium doped laser and the output beam is found be collimated with uniform phase [9]. The setup is such that the laser beam is made to enter the optical fiber coupler. The light that enters is thus split into two beams having the same intensity which travel along the single mode fiber coil in opposite directions. The output beam is then detected by then detector at the receiving end.

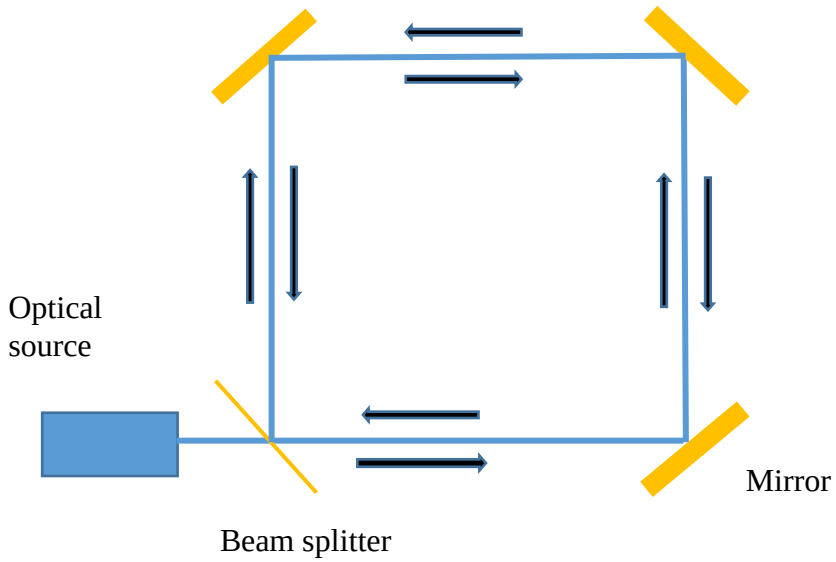

Figure 5: Sagnac interferometer

Figure 5 shows the schematic representation of a Sagnac interferometer. This specific configuration has been prevalently used in rotation sensing. In non-rotating configuration, both the clockwise (CW) and counterclockwise (CCW) modes are in phase with each other whereas in a rotating configuration, the optical path is shorter for one of the modes due to change in rotation velocity [9]. The interference pattern that is formed is dependent on the angular frequency of the setup. This is because of the Sagnac effect. When the orientation of the optical fiber coil is along the optical fiber coil axis, the phase difference between the two modes can be deduced using the formula

$$\phi = 8\pi NA\Omega/(\lambda * c)\ [9]$$

Where λ is the free space optical wavelength, N is the number of turns of the coil, A is the area of the Sagnac coil, Ω is the angular velocity and c is the velocity of light in free space. Sensitivity can be measured as the ratio of phase difference to the angular velocity which is given by,

$$S = 8\pi NA/(\lambda * c)$$

From the following formula, it can be seen that the sensitivity can be increased by increasing the coil radius, length of the fiber and frequency of the laser [9]. Factors that can possibly restrict the fiber length and coil radius would be optical fiber loss and packaging criteria limit respectively [9]. Sagnac fiber interferometers are found to be extremely useful in sensing time varying phenomena [9]. They have been studied extensively because of a lot of advantages such as simple fabrication and robustness. Hence, they prove to be one of the significant tools in detecting acoustic waves, strain, current and temperature [9].

1.4.3.3.2. Mach-Zehnder interferometers

Several advances in the fiber optic networks have been realized by the application of Mach Zehnder interferometers in diverse fields. The devices based on Mach Zehnder interferometers have been mainly used in switching, modulation, multiplexing of signals in optical communication thus offering high amplitude, high bandwidth responses over Gega hertz range [10].

Also, this configuration has been used in studies related to heat and mass transfer in fluids. It has been primarily used to measure the phase shifts that occur between two beams because of a sample present along their path or change in the path length. Mach Zehnder interferometers have thus been extensively used in a wide range of applications [10].

The optical setup is such that the beam splitters and mirrors which form the major optical components, are inclined to the direction of the beam at an angle of 45 degrees [10]. When the incoming collimated beam reaches the first beam splitter, it is divided

into two transmitted and reflected beams. Now, the transmitted beam is referred to as the test beam and the reflected beam is called the reference beam.

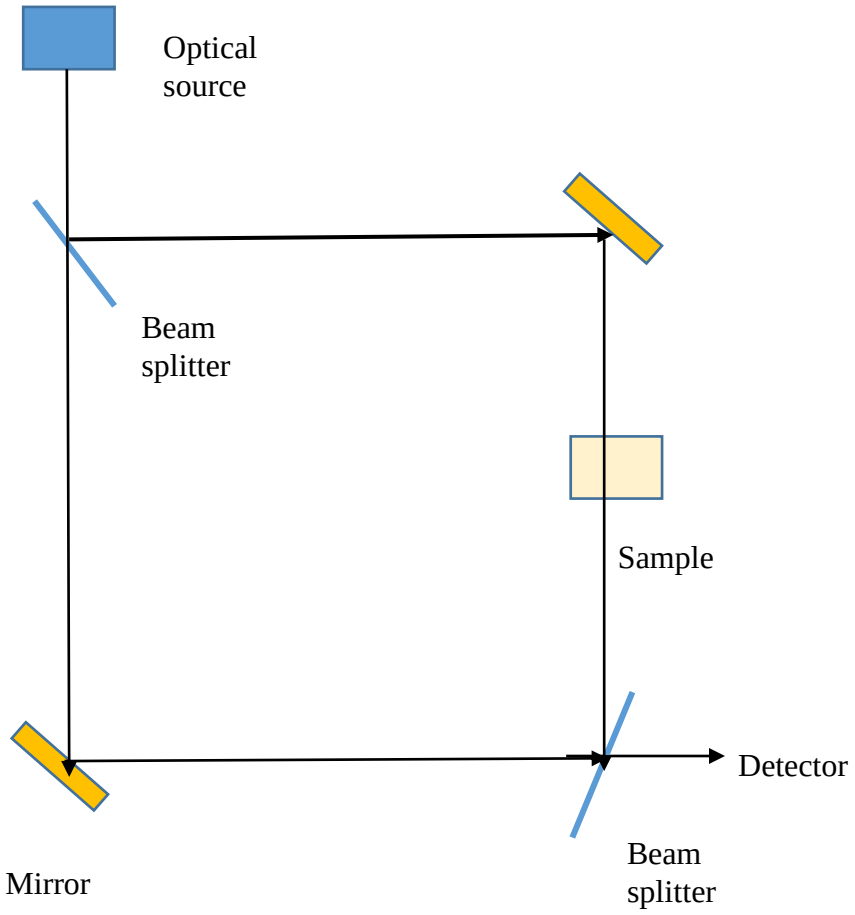

Figure 6: Mach Zehnder interferometer

Figure 6 shows the schematic representation of a Mach Zehnder interferometer. Initially, when the test beam passes through the test region, it is reflected by the first mirror and is reunited with the reference beam when it reaches the second beam splitter. The reference beam gets reflected when it passes through the second mirror. It travels through the reference medium and combines with test beam at the second beam splitter. Thus the two beams are superimposed such that it results in an

interference pattern. This pattern is helpful in examining the changes in refractive index in the test region [10].

In order to use this configuration for sensing applications, only test beam is exposed to external variations. Hence, any variation in the test arm that is influenced by external factors like strain, pressure, temperature can be evaluated by examining the variation in the interference of the signal. Fringe localization is one of the major characteristics that is found exclusively in Mach Zehnder interferometers [10]. Thus, this configuration can be utilized to function in two modes, the infinite fringe setting and the wedge fringe setting.

In infinite fringe mode, the geometrical path lengths are controlled such that the test and the reference beams have identical path lengths. The interference fringes are formed due to changes in refractive index. Each line in the fringe pattern is of constant phase and refractive index. The thickness of the fringes is inversely proportional to the local refractive index gradient [10]. It is usually used in the measurement of high refractive indices.

In wedge fringe mode, the optical components, namely, the mirrors and the beam splitters are misaligned on purpose to produce an interference pattern consisting of straight lines. When a refractive index disturbance is included in the test beam, these fringe lines get deformed and constitute the refractive index profiles in the fluid.

Mach-Zehnder interferometers are used as fiber optic sensors due to the fact that the phase difference can be controlled and manipulated by changes in environmental effects such as strain. Environmental changes affect the light wave in the cladding more than the core as the cladding portion of the fiber is found to be more sensitive than the core [10].

A long period grating (LPG) which is designed to guide the light from cladding to the core and vice versa is appropriate to be used in Mach Zehnder interferometry [9, 11]. The LPG couples the part of the beam guided at the core mode of the single mode fiber to the cladding of the same fiber, and another LPG recouples the beam to the core [12].

With extensive applications of Long Period Gratings (LPGs), Mach Zehnder interferometers have been used in inline waveguide configuration. Interference is usually caused by the uncoupled and the combined beam in the core. In inline type of interferometers, physical lengths in both reference and test arms are the same but vary in optical path difference due to modal dispersion [12]. LPG has lower cladding mode effective index than that of the core mode. Most of the inline MZIs are based on multimode interference. The cladding portion of the single mode fiber (SMF) is a multimode waveguide and hence the MZIs use multiple cladding modes. The sensing performance of multiple cladding mode MZIs is affected due to the fact that the sensitivity of each mode to external variations is different.

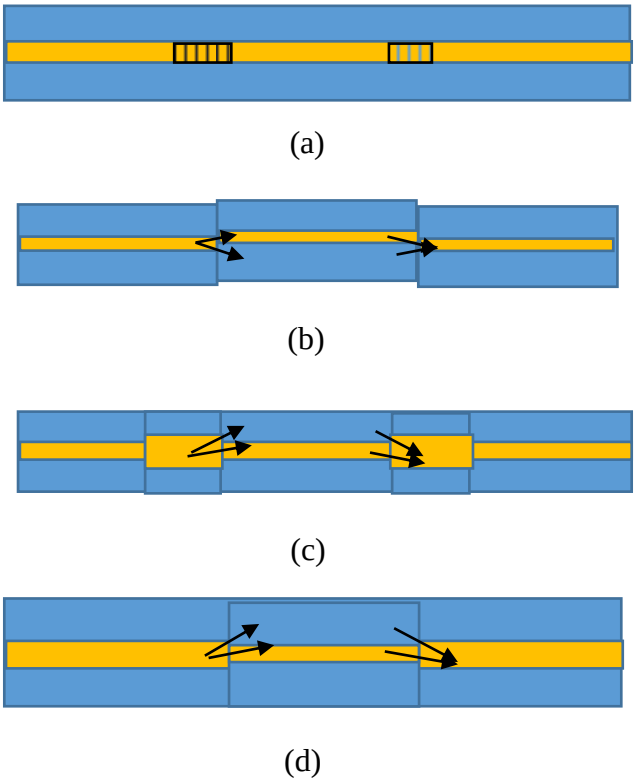

Figure 7: Configuration of various types of MZIs

The methods of using (a) a pair of LPGs, (b) mismatch between the cores of the fibres, (c) air-hole collapsing of PCF, (d) MMF segment, (e) small core SMF

Figure 7 shows the configuration of different types of Mach Zehnder interferometers. From Figure 7(b), we can see that beam is split into core and cladding modes by splicing the two fibers with minimum offset. Hence, we see that there is coupling of a part of the core mode with several cladding modes without any major effect on the wavelength. However, the number of cladding modes and the loss incurred can be controlled by monitoring the offset. Also, the beam can be split by splicing two fibers of different core sizes (figure 7(c, d)) [12].

When a multimode fiber is spliced between two single mode fibers, the light through the core of the single mode fiber is spread at the multimode fiber region and then recoupled with the cladding and core modes of the SMF (figure 7(d)). Also, a small core fiber can be spliced between two single mode fibers. This results in the beam entering the small core region being guided not only to the core as well as to the cladding region [13]. By gradually decreasing the thickness of the ends, the portion of the beam that is being guided towards the core can be coupled to the cladding region as the diameter of the core mode is increased. Apart from these, Mach Zehnder interferometers also utilize double cladding fiber, twin mode fibers and micro cavities in their configuration to produce interference [12].

1.4.3.3.3. Michelson interferometers

This configuration was invented by A.A.Michelson. It was designed based on the interference principle used in Young's double slit experiment. Michelson used his design to test the existence of ether, a hypothesized medium which allowed the propagation of light [12]. But the results were not satisfactory to be considered as a viable hypothesis. However, this configuration has also been used many other applications such as measurement of the wavelength of light, to detect and measure small changes in displacement during the propagation of light and in determining the change in the optical properties of materials [12].

The experimental setup of a Michelson interferometer is shown in figure 8. The beam splitter that divides the light beam (usually laser light) into two beams, each with equal intensity. One of the beams is transmitted to the movable mirror and the other is reflected towards the fixed mirror.

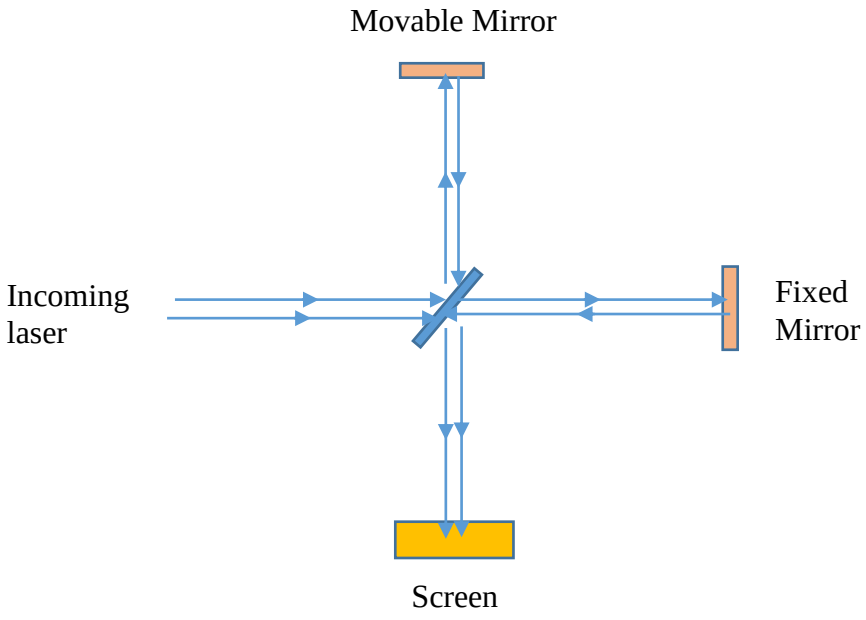

Figure 8: Setup of Michelson interferometer

Half of the light signal from the movable mirror is reflected from the beam splitter to the viewing screen. The other half of the light signal from the fixed mirror is transmitted to the viewing screen through the beam splitter. Since the two beams are from a highly coherent laser source, the phases are highly correlated. Due to the optical path difference between the two beams, there is phase difference between them. By changing the position of the movable mirror, the path length of one of the beams can be varied. In the presence of lens between the beam splitter and the laser source, a characteristic pattern is seen due to interference as bright and dark fringes on the viewing screen.

Michelson interferometers are similar to Mach-Zehnder interferometers with respect to methods used for the fabrication and principle of operation. However, Michelson interferometers are different due to the presence of reflectors.

Hence, the usage of reflection modes makes the configuration easy to handle in practical applications. Also, the capability of multiplexing in the presence of parallel connection with sensors is one of the key advantages of Michelson interferometers.

Many fiber optic sensors have been designed using the inline configuration of Michelson interferometers for the detection of temperatures and refractive indices of fluids [12-18]. Also, Michelson interferometers are being used for the measurement of flow velocity [18]. The configuration was modified where in tapering technique was used to divide the beam so that they propagate through the two cores of a twin-core fiber. The optical path difference between the two beams in the core was measured by the flow velocity sensor [18]. The bending of the fiber that was influenced by flow in turn affected the path difference [18].

1.4.3.3.4. Fabry-Perot interferometers

This configuration comprises of two surfaces that are parallel to each other and separated by a distance. Interference is caused by multiple and repeated superimpositions of the transmitted and reflected beams at the parallel surfaces [19]. Fabry Perot optical fiber interferometers (FPI) have been designed by placing the reflectors on the inside and outside the fibers. FPI sensors can be classified as extrinsic and intrinsic type sensors. The operation of extrinsic FPI sensor is based on the reflections formed in an external cavity. Figure 10(a) shows an extrinsic FPI sensor wherein the air cavity formed is supported by an external structure. This type of the Fabry Perot configuration uses high reflecting mirrors because of which it has the ability to produce interference signals. Also, it is comparatively much cheaper than other configurations and uses low cost equipment in its design. However, it has its own drawbacks of low coupling efficiency, packaging problem and careful

alignment [20]. The intrinsic type sensors have their reflecting modes within the fiber. Figure 9 shows the diagrammatic representation of extrinsic and intrinsic FPI sensors.

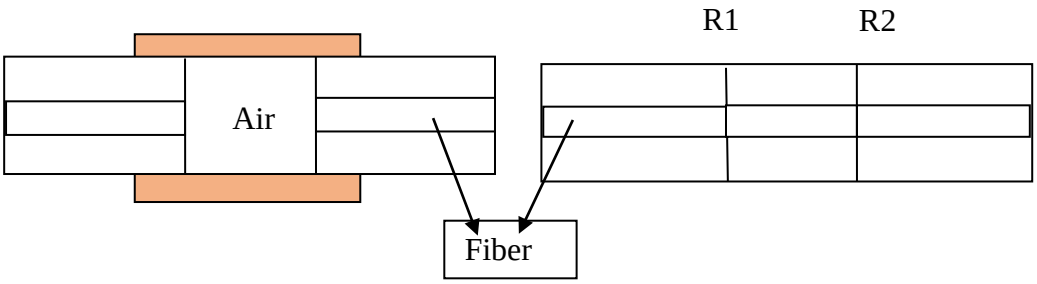

Figure 9: Types of FPI sensors

(**a**) Extrinsic FPI sensor (external air cavity seen), and (**b**) intrinsic FPI sensor consisting of two reflecting components, R1 and R2, along a fibre

The design of the cavity in the intrinsic type of interferometers is done using techniques such as chemical etching, micro machining, Fiber Bragg gratings and so on. However, they have a disadvantage of high fabrication costs. The spectrum of the Fabry –Perot interferometer shows intensity modulation of the wavelength dependent input beam [12]. This is because of the phase difference of the two transmitted and reflected beams. The phase difference is determined by

$$P = (2\pi / \lambda) * (n * 2 * L)$$

Where λ is the wavelength of light, n is the refractive index of the cavity and L is the length of the cavity [12]. Optical path difference variations, changes in physical length and refractive index of the cavity have resulted in changes in phase difference. The spacing between the two adjacent peaks in the interference spectrum is called as the free spectral range and is affected by variation in optical path difference. When the optical path difference is short, it results in a large free spectral range. Also, a large spectral range thus results in poor resolution. Hence it is mandatory to design and control these parameters for specific applications. The extrinsic type has the

advantage of detecting changes in displacement as the phase of the Fabry Perot Interferometric signal is directly influenced by changes in displacement of the external reflecting surface. FPI sensors have the potential of being used extensively as pressure and ultrasound sensors in extrinsic configuration by using thin polymers as reflecting surfaces [12].

1.4.4. Multimodal interference

The suitable configuration for the phenomenon of multimode interference (MMI) to occur is the SMS (SMF-MMF-SMF) configuration. This structure is obtained by splicing the MMF segment between two SMF segments [21]. Principle of multimode interference is that when light passes through the MMF segment, several modes of the MMF segment will be excited resulting in interference between them [21]. The SMS configuration is commonly preferred for refractive index sensing.

Self-imaging is a property of multimode optical fibers by which the input light field is reproduced at regular intervals along the direction of propagation of the light through the optical fiber. Due to this self- image effect, light field condensation in a particular plane results from constructive interference between the guided modes of the MMF segment [22].

1.4.5. Applications of fiber optic networks

Over the years, there has been a large growth in the field of fiber optic communication, especially with the use of interferometers in science and technology applications. They have been promising in delivering good and efficient results wherein they are being incorporated in the design of band pass filters in optical communication networks for inline signal processing. They have been used in novel

applications like oil leakage monitoring, depth measurement in oceanography and temperature measurement.

Also, interferometers have been extremely useful for bio sensing applications. They can effectively detect and measure the refractive index changes in fluids and liquids, because of which these devices have been used in quantifying minute changes in the concentration of toxins, proteins, whole cells and viruses. Some of the biological applications of interferometers have been discussed in this section.

1.4.5.1. Bio sensing applications

Development of biosensors is primarily inspired by everlasting need of simple, fast and live monitoring methods in various areas such as medicine, pharmaceutics, biologics, biotechnology and food processing.

Fiber optic biosensors measure absorbance to detect any changes in the concentration of the samples that absorb light of desired wavelength. Optical biosensors have been commonly used as pH and oxygen sensors for biomedical applications.

The pH sensor was designed such that the change in absorption occurs due to the presence of an absorptive indicator compound with an absorption peak of 625nm [23]. The sensor interacted with a red LED and the dichroitic mirror splits the wave into short and long components. These short and long signals were detected by the respective photodiodes and their currents were used to produce the output signal. From the observations done during the experiments, the sensor could provide accurate resolution and response time of about 0-40s [23]. After sterilization was done using gamma radiation, the sensor was tested with heparinized blood and its performance was in good agreement with the conventional blood gas analyzer [23]. Good

performance standards, reliable costs and easy construction are one of the key features of this design.

It was found that after the stimulation of UV radiation, the oxygen sensor's viologen indicator was found to be strongly absorbant. It returned to its transparent state after a brief amount of time. The rate at which the indicator returned to its transparency state was found to be proportional to the local concentration of oxygen. The absorbance of the indicator was monitored by red LED [23].

Fiber based infrared sensing has been one of the emerging and developing techniques for detecting organic and biological species. The sensor design was based on a mechanism wherein there is absorption of electric field and it propagates on the outer surface of the fiber interacting with any absorbing species present on the interface [23]. Because of the fiber geometry, large number of reflections occurs internally and leads to increased sensitivity. These optical fibers transmit infrared radiations in the spectral range of 400 to 4000 cm^{-1} and thus organic chemicals and biomolecules exhibit high vibrational spectrum in this spectral region [23]. This technique is called the fiber evanescent wave spectroscopy (FEWS) and has been widely used for the detection of pollutants and a wide variety of chemicals [23]. Mid infrared fiber optic neurotoxin bio sensors which are being widely used for the characterization of biological samples, were constructed by the usage of biologically active infrared transmitting chalcogenide fiber [24]. The fiber optic probe was exposed to various concentrations of neurotoxin. Infrared difference spectroscopy was performed before and after the exposure of the probe to different neurotoxin concentrations. In this way, binding of the receptor protein onto to the surface was monitored. Signals that were recorded and measured as a result of chemical changes due to interactions were in

good agreement with the standard and established kinetics of the receptor [18-23]. Fibers functionalized with enzyme films can be used as chemical sensors by using a reactive enzyme to functionalize the fiber and this enzyme can serve as a catalyst for chemical reactions [23].

A new and an interesting approach was used by researchers in detecting the interaction of molecules by using the colorimetric resonant diffraction grating for surface binding [25]. There were observations being made that when the surface grating was exposed to white light, only one wavelength was reflected. But when the organic molecules were bound to the surface of the grating, there was a shift in the wavelength due to change in optical path of light that was coupled to the grating. It has been studied that the complementary receptor molecules can be easily detected without the usage of fluorescent labels by just linking the molecules that function as receptors to surface of the grating. This technique could be employed by either immersing or drying the surface of the grating in the fluid. It had the ability to resolve changes of around 0.1nm thickness of protein binding [23, 25].

1.4.5.1.1 Enzyme based biosensors

Over the years, enzymes have been one of the most common biological components used in fiber optic biosensors. This is because of two main reasons:

1. Their ability to catalyze a number of reactions
2. They have the ability to detect a large number of analytes.

Fiber optic enzyme based sensors were developed for the detection of flurophore NADH [26-28]. Glutamate, being a neuro transmitter molecule, its quantity can be measured by using a submicron fiber optic sensor that consists of glutamate dehydrogenase which is directly immobilized by covalent bonding [26]. The NADH

fluorescence is detected and monitored during the reaction of enzymes which mediate the reaction between NAD^+ and glutamate. The response time of the fiber optic sensors were found to be extremely fast of the order of 50ms and thus had the potential to monitor the release of glutamate ions in brain cells [27, 28].

1.4.5.1.2. Detection of lipoproteins using optical biosensors

Concentration of lipoproteins in blood has been one of the important parameters as it is the carrier of cholesterol. Medical studies show that the reduction of cholesterol will result in decreased risk of heart diseases. However, there are theories and facts that show that the information about the cholesterol content is not sufficient to determine the risk of cardiovascular diseases. The size, shape, and the configuration of lipoproteins hereby play a very important role and optical fibers have thus been able to deliver good results. The arterial lesions can thus be investigated in-vivo using optical fibers. Fluorescence microscopy with optical fibers in this regard, helps in capturing intimal images of arteries [25].

1.4.5.1.3. Fiber optic sensors used in bacterial detection

Fiber optic biosensors have been considered as one of the most commonly used tools to detect pathogens, toxin molecules and various bacterial substances. An antibody-Aptamer functionalized fiber optic sensor was developed to detect listeria monocytogenes from food. Fiber optic sensor was employed with an invasin protein of L. monocytogenes. This sensor was sandwiched with an antibody. Optical fiber that was coated with streptavidin was immobilized with Polyclonal anti Listeria antibody. This was used in capturing bacteria. The bacteria were successfully detected by the sensor in pure culture as well as in the presence of other bacteria [29].

1.4.5.1.4. Optical fibers coated with chitosan used as nickel mediated protein assembly

Optical fibers were coated with chitosan were used to demonstrate that nickel can mediate protein assembly [30]. The optical fibers were incubated in a bath containing aqueous solution of sodium chloride and 20% ethanol. The fibers were later rinsed with $NiCl_2$ solution for about an hour at room temperature. These nickel functionalized fibers were treated with 5% not fat milk to block the non-specific binding of proteins (either His GFP or protein G).

After blocking, the proteins are then incubated in solutions containing these His tagged proteins. Results showed that Ni^{2+} binds to the protein assembly and in this way, this study demonstrated that the amino polysaccharide along with Nickel solution could be used to evolve as major biofunctionalised assemblies and they can be used to form fibers that can be a part of protein assembly mechanisms [30].

1.4.5.1.5. Long period grating sensors for hemoglobin (HgB) sensing

A lightly etched long period grating sensor was used to measure the hemoglobin concentration in sugar solution. Initially, solutions with different hemoglobin concentrations were prepared by adding HgB to water. A known quantity of these solutions was added to sugar solutions.

When fabricated long period grating sensors were immersed in these solutions, there was a shift in the wavelength which was recorded. The plot of HgB concentrations versus the wavelength provided a sensitivity of 20nm/1% change in HgB concentration [31].

1.4.5.1.6. Fabry Perot Interferometry based immunoassay sensor

Interferometers have been used in immunological studies as immunoassay sensors. The setup consisted of fiber optic sensors functionalized with PDMS which thus led to the modification of the tip assembly. As the sensor tip was immersed into the target solution, immunoreaction took place which led to covalent binding of antigen antibody molecules. In this experiment, rabbit IgG and anti-rabbit IgG-Cy3 were covalently bounded which led to the variation of refractive index at the interface along with changes in reflectance [32]. The sensitivity of the immunoassay was found to be 10^{-12}g/ml. This immunoassay sensor has found applications in in-vivo and in-situ monitoring of reactions in neurocytes [32].

1.4.5.1.7. Fiber optic biosensors used in the detection of Clostridium botulinum.

Clostridium botulinum is an anaerobic, spore forming bacterium that has the ability to produce neurotoxins [32]. The designed fiber optic sensor could detect the toxin even at low concentrations of 5ng/ml. Optical fibers were cut at desired lengths and the ends were connected to connectors. The ends were polished and roughened by placing the fiber ends in a 3:1 mixture of hydrochloric acid and nitric acid for about seventeen minutes.

The cladding at the distal end of the fiber was stripped off and was gradually tapered by immersing the cladding free portion in hydrofluoric acid. The fiber ends were cleaned for immobilization of affinity purified anti-A antibodies. Results showed that affinity purified anti toxin A antibody detected the toxin concentrations as low as 5ng/ml [32]. Thus the design was employed for rapid, specific detection and real time analysis in detecting Clostridium botulinum toxin [32]. Fiber optics has thus, been one of the unique and emerging techniques for specific detection of toxins.

1.4.5.1.8. Selective nitric oxide biosensor

The development of fiber optic biosensors that were selective of nitric oxide explained the preparation of sensors with cytochrome c protein [33]. The response time was found to be less than 1s and the detection concentration was as low as 20 micrograms/ml. The sensor was fabricated using multimode fibers that were salinized for 2 hours in 200 µL 3-(trimethoxysilyl) propyl methacrylate [33]. The pH was adjusted at 3.5 and was dissolved in water. The fiber was rinsed with pH 3.5 HCl/H_2O after salinization.

One milligram sample of the protein C. vinosum cytochrome c' was mixed with h 200 µL of acrylamide-bisacrylamide solution [33]. Following this, the tip of the sensor was placed inside the solution and photopolymerised using 488nm light from argon laser. The sensor was then kept immersed in saturate nitric oxide solution in 10 mM pH 7.4 phosphate buffer [33].

The excitation and absorbance spectrum of the fiber optic tip was studied and the selectivity of the sensor to nitric oxide was demonstrated. These sensors have also been used in detecting macrophages that produce micro levels of nitric oxide when stimulated by type II interferons, IFNγ [33].

1.4.5.1.9. Detection of biological analytes.

Over the decades, a lot of research and studies are being done in the field of sensors used for bio-sensing applications. The sensor constituted of a photoluminiscent structure that was embedded in a sensor hydrogel supported by substrate hydrogel [34]. The photoluminiscent structures comprise of a class of nanostructures which may include carbon nanotubes, nanowires, quantum dots, etc. [34].

The hydrogels being used are polymers that are porous in nature, thus facilitating access to analytes to be embodied to the components of the hydrogel. Examples of hydrogels include polyacrylamides, polyvinyl alcohol and other copolymers with abundance of hydrophilic groups.

The photoluminiscent structures also constitute linker polymers [34]. These linkers are found to bind to the surface of optical fibers by means of either ionic, covalent, dipolar or hydrogen bonds. Most commonly used linker molecules are dextran and chitosan. The interaction between the protein and linker deals with the binding of the linker molecules to the capture proteins. The binding is configured with the help of a first binding partner in the linker that helps in interaction of the linker with the capture protein. The first binding partners are usually metal ions and some of the common examples include nickel, copper, cobalt, mercury, cadmium etc [34]. The linker molecules consist of chelation region wherein the chelator (linker molecules) binds to the first binding partner.

These linker molecules interact with the capture protein which constitutes a second binding region. The first binding partner (metal ions) and the second binding partner bind together and thereby chemically reacting with the protein molecule. The second binding partner is usually a His protein tag, a DNA sequence with six to nine Histidine residues that are used in vectors for the production of recombinant proteins.

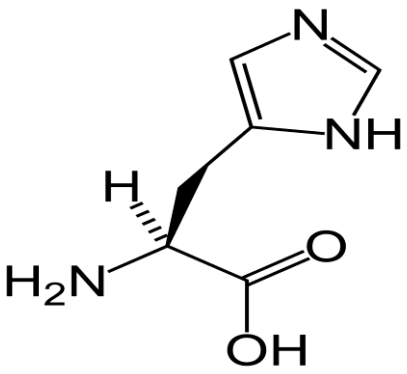

Figure 10: Structure of histidine [35]

The structure of histidine is shown in Figure 12. These Histidine residues are added at the N or C terminus of the coding sequence of the protein of interest. The choice of adding these His tags to N or C terminus depends on the characteristics of proteins [35].

Most commonly used technique of adding polyhistidine residues is by PCR technique wherein primers are designed such that they have repetitive histidine codons (CAT or CAC) just after the START or the STOP codon [35].

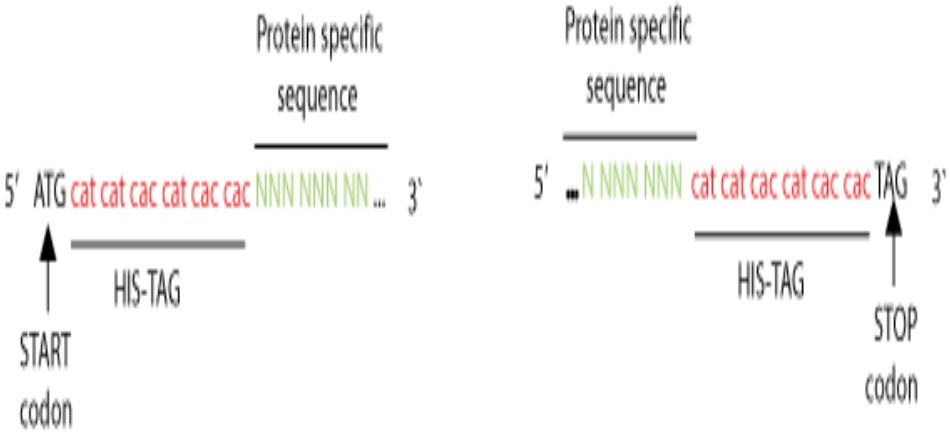

Figure 11: His Tag primers [36]

His tagged primers used in the purification process of recombinant proteins are shown in Figure 13. The important advantage of using these His tagged proteins is that these Histidine residues have an affinity towards metal ions which form covalent bonds with the chelator [36].

Thus, they help in purification process of recombinant proteins .This technique based on the affinity of metal ions towards histidine residues in aqueous solutions is referred to as Immobilized metal ion chromatography (IMAC) [37]. Typical Ni NTA (Nitrilotriacetic acid) agarose resins are regarded as the chelating resins that aid in specific binding of metal ions to the His tags are used [37]. IMAC of proteins can be explained by the coordination of histidine residues. When the surface of a protein molecule provided with electron donating groups like histidine, cysteine or tryptophan is applied to a chromatographic column containing chelated and immobilized metal ions (IDA-Metal (II)) like Co, Ni, Cu, Zn, co-ordination bonds are formed thus leading to the retention of the protein molecule [38]. Figure 14 shows an example of how nickel ions bind to histidine residues of the protein molecule.

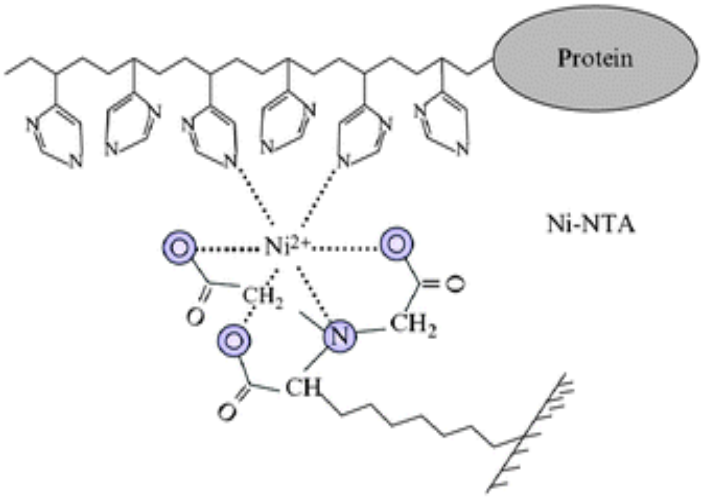

Figure 12: Nickel histidine binding [37]

The presence of more number of histidine residues resulted in increased affinity of metal ions to these histidine residues by coordination bonds. It was found that the retention of protein carrying multiple histidine residues in its adjacent positions at its surface was more pronounced and stronger than that of proteins with histidine residues which were far apart from each other [38]. This technique has been very useful by providing a variety of applications such as detection of recombinant proteins, drugs and biomarkers [36-38]. Self -assembled monolayer (SAM) was developed where in there was selective binding of proteins onto the monolayer. These proteins had their primary sequence terminating with His Tags [39].

Preparation of the self - assembled monolayer was done by the adsorption of protein molecules onto the gold surface made of a mixture of two alkenethiols [39]. One of them terminated with a Nitrilotriacetic acid (NTA) group and the other, terminated with triethylene glycol.

Histidines were bound onto the vacant sites of the Ni (II) ions that were chelated to the surface NTA groups. Experimental observations showed that the binding was specific for His tagged proteins and Ni (II) was essential for such binding to occur [39].

1.4.5.2. Other applications of fiber optic sensors

There has been a lot of development in the field of design and development of humidity based sensors. They are being used for many applications in day to day life such as for air conditioning purposes, environmental applications, industrial and chemical applications. Humidity based fiber optic sensors and polymer based and silica glass fiber based humidity sensors have proven to have advantages than the conventional electrochemical humidity sensors mainly because of their low weight,

capability to resist electromagnetic interference, small size and resistance and corrosion [39]. Fiber Bragg grating sensors functionalized with polymers have been widely used for humidity sensing. Polyamides are one of the best suited polymers due to their exceptional properties such as, high tensility, mechanical stability, adhesiveness and heat resistance [40].

Functionalization process is usually carried out by dip coating technique wherein a ten layer coating of polyamide is formed. The average thickness of the polyamide functionalization is found to be around 35 micrometers. When this polyamide layer is functionalized on the optical fiber to form a layer that is sensitive to moisture, the water molecules tend to accumulate on the sensor and result in shift of wavelength. Based on this shift in Bragg wavelength, humidity measurements are carried out using spectral analysis [40].

1.4.6. Advantage and drawbacks of fiber optic biosensors

1.4.6.1. Advantages

1. Optical fibers help in long distance transmission of light over long distances and thus there is no requirement of the bio-receptors to be in close proximity with the optical fiber. This characteristic feature of optical fibers thus helps in various noninvasive configurations.

2. Fiber optic biosensors have multiplex capability. They have the ability to analyze and determine multiple or single analyte concentrations within a single central unit. This is because of the fact light of different wavelengths can be guided in optical fibers in different directions.

3. One of the striking advantages of optical fibers is their capacity to have immunity towards electric and magnetic interference.

4. They are found to be manufactured at a very low cost and in miniaturized setups. Also, since they are biocompatible, optical fibers are used in in-vivo applications.

5. Optical biosensors offer tremendous applications in the field of environmental pollution control [1, 10].

1.4.6.2. Drawback

There is a possibility of interference of ambient light that can affect the performance of optical fiber biosensors. However, this can be eliminated by the usage of light isolation sources.

2. EXPERIMENTAL

2.1. Materials and methods

Preparation of Glycerol solutions

Glycerol solutions of different refractive indices were prepared for the characterization of the sensor. Glycerol having a refractive index of 1.473 RIU and water having a refractive index of 1.33 RIU was used in the preparation glycerol solutions and a refractometer (Model AL-PAR) was used to measure the refractive indices of these solutions. The refractive index of the solutions was varied by the addition of the different concentration of the glycerol. Characterization of the sensor was done to study the sensitivity of the sensor to different refractive indices.

When the sensor was immersed in solutions of different RI, the wavelength dips in the transmission spectrum shifted towards the longer wavelength when the surrounding RI value increased [41]. The shift in the transmission wavelength dips was due to the propagating core and cladding modes in No Core Fiber [42]. Figure 13 shows the RI calibration curve for the fabricated No Core sensor wherein dip shift is plotted against refractive index.

.

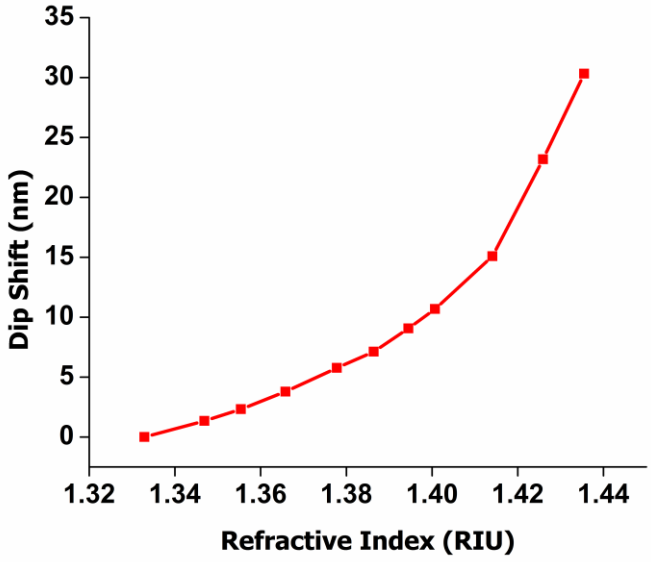

Figure 13: RI calibration curve

Preparation of Piranha solution

Piranha solution is a mixture of sulphuric acid and hydrogen peroxide that is used on substrates to remove the organic residues present. Typically 98% sulphuric acid solution and 30% hydrogen peroxide is mixed in the ratio 3:1. Hydrogen peroxide solution and 98% sulphuric acid solution is obtained from Sigma Aldrich and used as received. Piranha solution is prepared by adding hydrogen peroxide to sulphuric acid slowly and mixing them. Care is taken to ensure that the temperature doesn't rise too much as the mixture of solutions can get extremely hot.

Preparation of PBS buffer

Phosphate buffer saline (PBS) is water based solution constituting sodium phosphate, sodium chloride and some quantities of potassium phosphate and potassium chloride. It is nontoxic and isotonic.

10x PBS was purchased from Merck and used as received. 30 ml 1x PBS buffer is prepared by the addition of 27ml of Millipore water and 3ml of 10x PBS buffer (ratio 1:9) and mixing the solution thoroughly using the mixer.

Millipore water is described as ultrapure water of type 1 according to ISO 3696[43]. Purification process involves various filtration and deionization processes to the desired degree of purity typically characterized by resistivity (18.2 MΩ·cm at 25 °C) [43].

Preparation of Ni/Chitosan solution

Chitosan is a linear polysaccharide consisting of ß-(1-4)-linked D-Glucosamine and N-acetyl glucosamine units that are randomly distributed. It is obtained by the deacetylation of chitin, a structural element forming the exoskeleton of crustaceans. Nickel (II) Chloride, Chitosan and acetic acid are purchased from Alfa Aeser, Aldrich and Fluka respectively and are used as received. 2% Chitosan is prepared by dissolving 2g of Chitosan in 100ml, 4% acetic acid solution and is magnetically stirred for 24 hours at room temperature till all the solute is dissolved. 0.1 g of dry nickel chloride powder was added to a glass toppered flask containing 20 ml of 2% chitosan solution and are continuously stirred using a magnetic stirrer for 24 hours.

Preparation of different concentrations of trypsin sample

Trypsin is a serine protease that is mainly involved in the protein breakdown into smaller peptides. Trypsin is produced in the pancreas in inactive form as trypsinogen. It facilitates in cleaving the peptide chains mainly at the carboxyl side of amino acids, lysine or arginine, except when either of them is bound to proline at the C terminal.

For the experiment, the stock solution of 30 ml of 200µg/ml of trypsin sample was prepared by dissolving 0.006 grams of trypsin in 30ml of 1x PBS Buffer and mixing

thoroughly using the mixer. This stock solution was diluted to obtain the desired concentrations of trypsin solution by serial dilution.

2.2. Fabrication of the sensor

A No core fiber optic sensor (NCF) was fabricated by splicing a 2 cm long No core fiber with two Single mode fibers at both the ends. The splicing of the optical fibers is done use the fusion splicing technique.

The ends of two single mode fibers are first stripped off so that the outer jacket is removed and the fiber ends are cleaned thoroughly with ethanol. The ends of the single mode fibers are then cleaved using the fiber cleaver. The no core fiber is then stripped off and cleaved so that we have 2cm of the stripped off portion that is free from the jacket. One end of the no core fiber is then fused with the single mode fiber using the arc fusion splicer (DCM fusion splicer 39). Similarly the other end of no core fiber is fused with another single mode fiber using the above procedure.

The ends of the fiber were examined by employing a viewer of the fusion splicer to ensure if the fiber ends are precisely cleaved. The electric sparks produced within the splicer are used to clean the area to be spliced. After the fiber ends are cleaned, an electric spark of a higher magnitude is used to allow the temperature of the fiber glass to be increased above its melting point. This leads to the fusion of two ends together. The location of the spark and its energy is controlled such that the loss of the light in the splice is reduced [44]. Thus, the No core sensor was fabricated.

2.3. Experimental setup

2.3.1. Functionalization of Ni-Chitosan film on the sensor

Before functionalizing the fiber with Ni-Chitosan film, the sensor is dipped in piranha solution for about 60 minutes. Piranha solution is usually used to wash away all the organic matter off the substrate. Also, it helps in adding hydroxyl groups (OH^-) to the sensor surface and to make them hydrophilic. The sensor is carefully taken out from the piranha solution and is kept immersed in Millipore water for 30 minutes. The sensor is then dried by carefully fuming the sensor with nitrogen for about 5 to 10 minutes. The sensor is placed in a channel created by two cover slips. The two cover slips with approximately 0.1mm thickness are attached to a glass slide that is about a millimeter thick in such a way that there is approximately 1mm gap between the cover slips and it forms a channel for the sensor to be placed inside the channel. Ni/Chitosan solution is carefully filled inside the channel with the sensor placed inside it. Figure 14 shows the glass slide setup for functionalization of the No core sensor with Ni-Chitosan film. The setup is then dried in the oven for about 12 hours at 40 degrees.

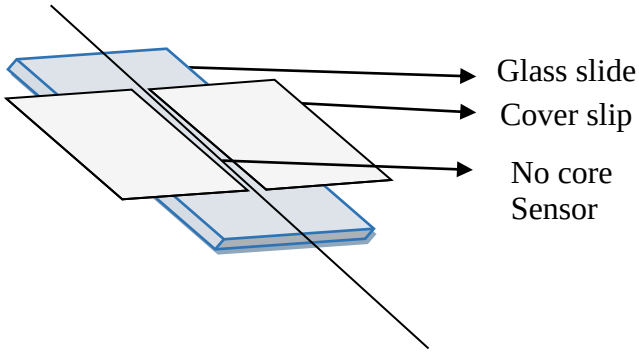

Figure 14: Glass side Setup for functionalization of the No core sensor with Ni-Chitosan film

2.3.2. Trypsin detection

After functionalization of the No Core sensor with Ni-Chitosan film, the sensor is kept immersed in 1x PBS buffer overnight. Figure 15 shows the diagrammatic representation of the sensor functionalized with Ni-Chitosan film.

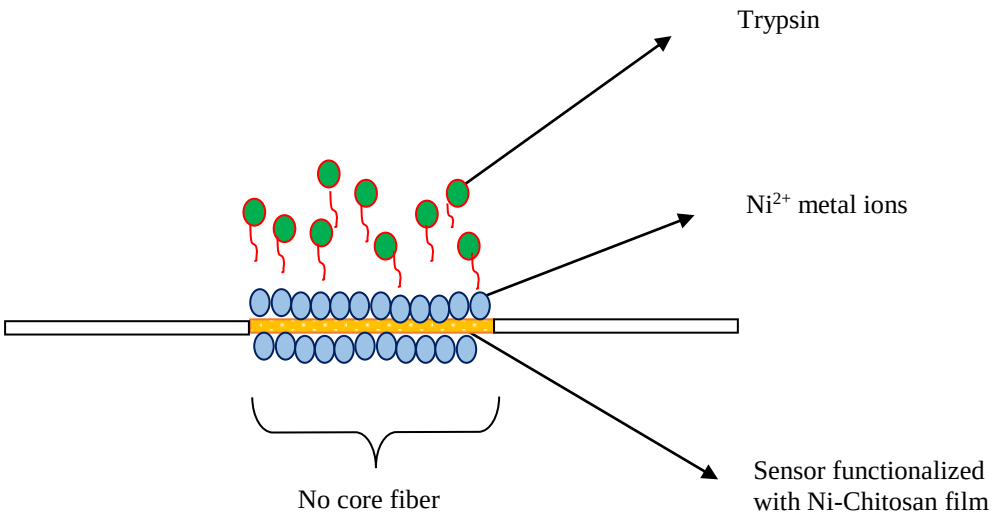

Figure 15: Diagrammatic representation of sensor functionalized with Ni-Chitosan film

The sensor is spliced with lead-in and lead-out SMFs and is connected to the broadband light source (Model: S3223-BA2) (through lead-in SMF) on one end and to the optical spectrum analyzer (Yokogawa AQ637) (through lead- out SMF) on the other end.

Figure 16 shows the experimental setup for trypsin detection.

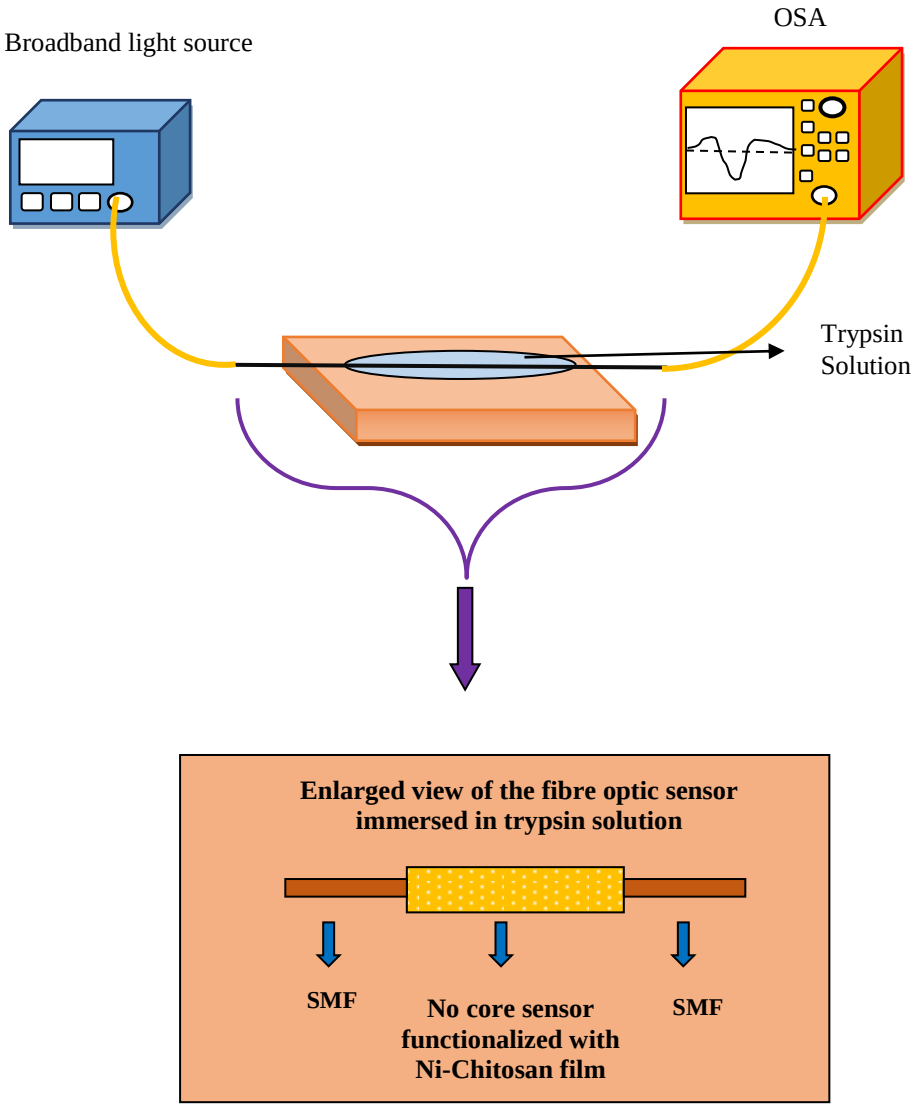

Figure 16: Experimental setup for trypsin detection

The sensor is carefully held in position using the fiber holders before placing it onto the translational stage. The sensor is kept immersed in 500 microlitres of each concentration of trypsin solution.

Sensor spectral response is recorded using the optical spectrum analyzer for every ten minutes till the spectral response displayed on the OSA is stabilized. The sensor is rinsed thoroughly in PBS (Phosphate Buffer Saline) buffer solution for about ten minutes before immersing the sensor in a different concentration.

3. RESULTS AND DISCUSSIONS

The fabricated No Core sensor was functionalized with Ni-Chitosan film. The Imaging software, NIS-Elements D was used to obtain the microscope images of the No core sensor functionalized with Ni-Chitosan film that were captured using the light microscope. The detection of trypsin by the functionalized sensor was carried out for different concentrations of the trypsin solution. The spectral responses of the sensor were plotted using OriginPro® and the sensitivity of the fabricated sensor was calculated.

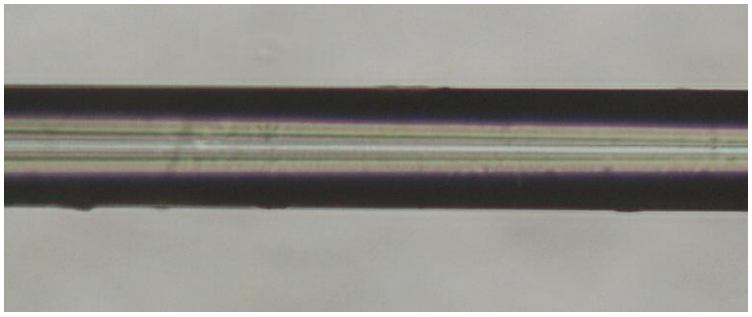

Figure 17: Microscope image of the bare No core sensor

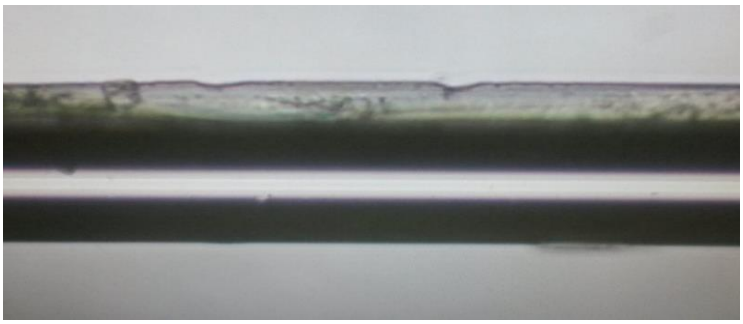

Figure 18: Microscope image of No core sensor functionalized with Ni-Chitosan film

Figure 17 and Figure 18 shows the microscope images of bare sensor and the sensor functionalized with Ni-Chitosan film, respectively. The images of the sensors captured from the light microscope were used to study the extent of functionalization. From figure 18, it is observed that the surface of the sensor is not clearly visible, due to functionalization, thus proving the presence of functionalization of Ni-Chitosan film on the sensor.

The detection of trypsin by the functionalized sensor was carried out for the following concentrations of trypsin sample: 2.5µg/ml, 5µg/ml, 10µg/ml, 20µg/ml, 40µg/ml and 200µg/ml. The sensor was kept immersed in 500 microlitres of each of these concentrations and the spectral response was recorded using the optical spectrum analyzer for every ten minutes.

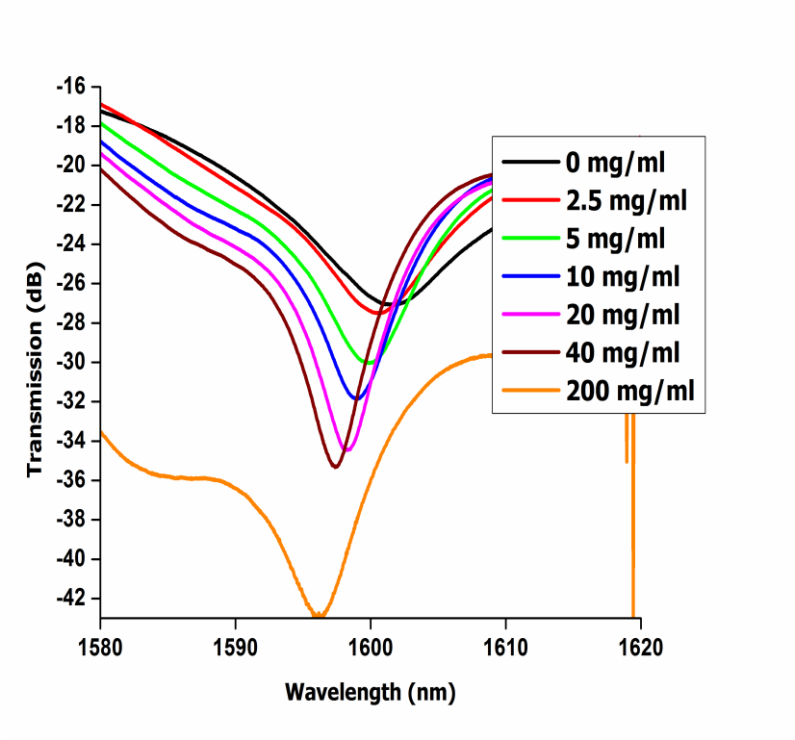

Figure 19: Sensor spectral response

Figure 19 shows the transmission spectrum response of the sensor for different concentrations of the trypsin sample ranging from 0 to 200μg/ml. These plots revealed significant resonant wavelength dip shifts for increasing concentration of protein sample. Figure 19 indicated that when the No core sensor functionalized with Ni-Chitosan film was immersed in the increasing order of different concentrations of trypsin, the transmission spectrum response showed resonant wavelength dips that shifted towards the lower wavelengths (blue shift).

Trypsin consists of residues of histidine-57, aspartate-102 and serine -195 at the active sites. When the sensor functionalized with Ni-Chitosan film is immersed in trypsin, the electron donating histidine residues of trypsin form coordinate bonds with nickel which results in the retention of the protein. The imidazole functional group of histidine is responsible for binding with nickel metal ion. The Nitrogen atoms present in imidazole functional group acts as electron donors. The strength of the retention of the protein increases with increased number of histidine residues in the protein that form coordinate bonds [45].

According to the principle of Immobilized metal ion chromatography (IMAC), binding of proteins to immobilized metal ions is based on the specific interaction between the electron donating group of the protein and the coordination site presented by the metal ion [45]. The affinity of proteins for metal is explained by the concept of hard and soft acids and bases which states that when two atoms are involved in the formation of a bond, one atom acts as a Lewis acid and the other, as a Lewis base. Ni^{2+}, being a transition metal ion is regarded as a borderline Lewis acid.

These transition metal ions, especially Ni^{2+} having a coordination number of six, electrochemical stability and borderline polarizability is found to be the most suitable transition metal ion to be utilized in IMAC [46, 47]. The theory of Hard and Soft Acids and Bases concept also states that the ligands to which the metal ions bind, can be classified as hard, soft and borderline bases and the ligands (histidine) containing aromatic nitrogen atoms are considered as borderline bases [48]. Nickel, thus binds favorably with aromatic nitrogen atoms (borderline bases) which are electron donating atoms present in the imidazole ring of histidine residues of trypsin. The binding of nickel ions to trypsin occurs at a neutral or a slightly basic pH at which the histidine residues are in deprotonated state [46, 47]. Based on this concept, when the sensor is immersed in desired concentrations of the trypsin sample, the nickel ions bind to trypsin resulting in transmission dip shifts towards lower wavelengths (blue shift) in the sensor spectral response. Nonspecific binding of nickel ions to endogenous proteins that consists of histidine clusters might occur, which can be removed by using elution buffers such as low concentrations of phosphate buffers, sodium chloride or imidazole [49, 50]. Elution buffers help in disrupting the interactions between the metal ions and the protein. This reduces the affinity between them and forces the metal ions to get back to their active phase. They play an important role since they wash away the unbound proteins and decrease the Non-specific off-target linkages [35, 37].

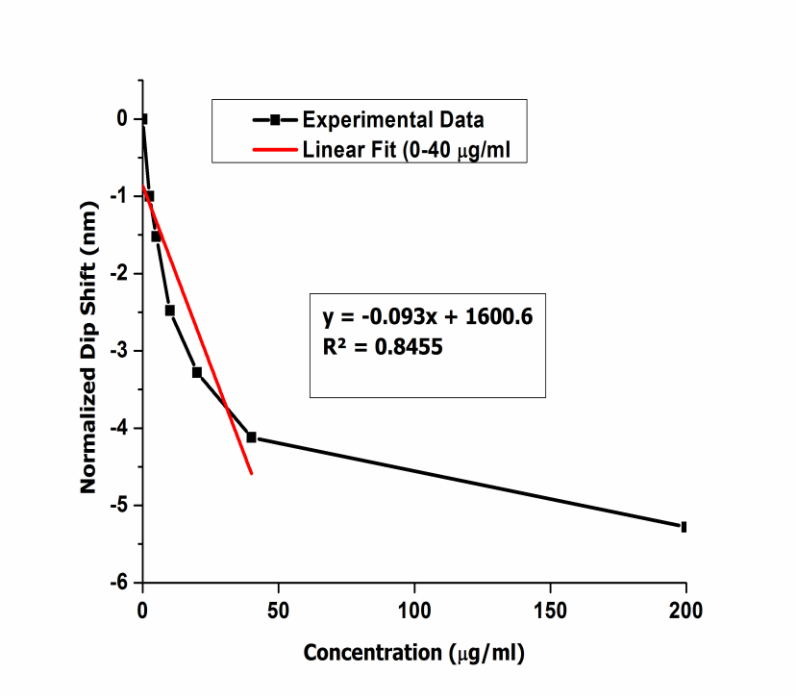

Figure 20: Sensor calibration curve

Figure 20 shows the calibration curve of the sensor wherein the normalized dip shift is plotted against concentration. From the above graph, R^2 is found to be 0.8455, thus confirming a good fit with respect to the experimental data points. From the linear regression equation, we determine that the slope of the linear fit line which indicates the sensitivity of the sensor is found to be -0.093 nm μg^{-1} ml^{-1}.

4. CONCLUSION

In this study, detection of trypsin by interferometry based fiber optic sensor has been demonstrated. The fabricated No Core fiber optic sensor was functionalized with Ni-Chitosan film. The nitrogen atoms present in the imidazole functional group of histidine residues of trypsin acted as electron donors thus forming co-ordinate bonds with nickel. The effective binding of Nickel ions to the Histidine residues of trypsin resulted in significant dip shifts towards lower wavelengths in the transmission spectrum when the sensor was immersed in different concentrations of the trypsin sample. These dip shifts revealed the binding of nickel ions to trypsin.

Interferometry based fiber optic sensors have been successful in providing promising advantages for medical applications such as in medical imaging, bio sensing, precise measurements, to mention a few. The application of the sensor design for sensing trypsin can be extended to diverse areas in field of pharmaceutics, detection and monitoring of antibodies, industrial and medical diagnostic applications [1]. This sensor offers important additional features such as immunity to electromagnetic interference, biocompatibility and small size, thus owing to be more advantageous than the current conventional electronic biosensors [1].

REFERENCES

1. Bosch, M. E., et al. (2007). "Recent Development in Optical Fiber Biosensors." Sensors (Basel) **7**(6): 797-859.

2. Gupta, B. and B. D. Gupta (2006). Fiber optic sensors: principles and applications, New India Publishing

3. Ghatak, A. and K. Thyagarajan (1998). An introduction to fiber optics, Cambridge university press.

4. Lin, M., et al. (2014). "All-Fiber Strain and Curvature Sensor Based on No-Core Fiber." Sensors Journal, IEEE **14**(5): 1514-1517.

5. Xia, L., et al. (2013). "Novel optical fiber humidity sensor based on a no-core fiber structure." Sensors and Actuators A: Physical **190**(0): 1-5.

6. Wang, B. S. and J. Stathis (2010). Technologies of fiber fusion and fused device fabrication for sensing applications.

7. Grattan, K. and T. Sun (2000). "Fiber optic sensor technology: an overview." Sensors and Actuators A: Physical **82**(1): 40-61.

8. Artur G. Olszak, J. S., and Monteith G. Heaton (2001). "Interferometric approaches each have advantages." from http://www.laserfocusworld.com/articles/print/volume-37/issue-9/features/interferometry/interferometric-approaches-each-have-advantages.html

9. Ali Reza Bahrampour, S. T., Marzieh Bathaee and Farnaz Farman (March 3, 2012). Optical Fiber Interferometers and Their Applications, "Interferometry - Research and Applications in Science and Technology". Ivan Padron, Intech

10. Verma, S., et al. "Optical Interferometers: Principles and applications in transport phenomena." Interferometry-Principles and Applications, Edited by Mark E. Russo, Nova Publishers, USA, ISBN: 978-971.

11. Dianov, E. M., et al. (1996). In-fiber Mach-Zehnder interferometer based on a pair of long-period gratings. Optical Communication, 1996. ECOC '96. 22nd European Conference on.

12. Lee, B. H., et al. (2012). "Interferometric Fiber Optic Sensors." Sensors **12**(3): 2467-2486.

13. Jing-Jing, Z., et al. (2010). "Fiber-Optic High-Temperature Sensor Based on Thin-Core Fiber Modal Interferometer." Sensors Journal, IEEE **10**(9): 1415-1418.

14. Tian, Z., et al. (2008). "Single-mode fiber refractive index sensor based on core-offset attenuators." Photonics Technology Letters, IEEE **20**(16): 1387-1389.

15. Kim, D. W., et al. (2005). "In-fiber reflection mode interferometer based on a long-period grating for external refractive-index measurement." Applied Optics **44**(26): 5368-5373.

16. Van Brakel, A. and P. L. Swart (2005). "Temperature-compensated optical fiber Michelson refractometer." Optical Engineering **44**(2): 020504-020504-020502.

17. Kwan Seob, P., et al. (2010). "Temperature Robust Refractive Index Sensor Based on a Photonic Crystal Fiber Interferometer." Sensors Journal, IEEE **10**(6): 1147-1148.

18. Libo, Y., et al. (2008). "A Compact Fiber-Optic Flow Velocity Sensor Based on a Twin-Core Fiber Michelson Interferometer." Sensors Journal, IEEE **8**(7):1114-1117

19. Vaughan, M. (1989). The Fabry-Perot interferometer: history, theory, practice and applications, CRC press.

20. Putman, M. A., et al. (1993). "In-line fiber étalon for strain measurement." Optics Letters **18**(22): 1973-1975

21. Jorge, P. A. S., et al. (2012). "Fiber Optic-Based Refractive Index Sensing at INESC Porto." Sensors **12**(6): 8371.

22. Socorro, A. B., et al. (2014). "Sensitivity enhancement in a multimode interference-based SMS fibre structure coated with a thin-film: Theoretical and experimental study." Sensors and Actuators B: Chemical **190**(0): 363-369

23. Russo, M. E. (2012). Interferometry Principles and Applications, Novapublishers

24. De Rochemont, L., et al. (1993). Evanescent-Wave infrared fiber optic biosensor. Fibers' 92, International Society for Optics and Photonics

25. Cunningham, B., et al. (2002). "Colorimetric resonant reflection as a direct biochemical assay technique." Sensors and Actuators B: Chemical **81**(2): 316-328.

26. Cordek, J., et al. (1999). "Direct Immobilization of Glutamate Dehydrogenase on Optical Fiber Probes for Ultrasensitive Glutamate Detection." Analytical Chemistry **71**(8): 1529-1533

27. Choi JW, Bae JY, Min J, Cho KS, Lee WH (1996) Sensor Mater 8:493–504

28. Zhang, W., et al. (1997). "Dual-enzyme fiber optic biosensor for pyruvate." Analytica Chimica Acta **350**(1–2): 59-65

29. Ohk, S. H., et al. (2010). "Antibody–aptamer functionalized fibre-optic biosensor for specific detection of Listeria monocytogenes from food." Journal of Applied Microbiology **109**(3): 808-817.

30. Shi, X.-W., et al. (2008). "Chitosan Fibers: Versatile Platform for Nickel-Mediated Protein Assembly." Biomacromolecules **9**(5): 1417-1423

31. Chen, X. (2013). "Optical Fibre Gratings for Chemical and Bio-Sensing."

32. Ogert, R. A., et al. (1992). "Detection of Clostridium botulinum toxin A using a fiber optic-based biosensor." Analytical Biochemistry **205**(2): 306-312.

33. Barker, S. L. R., et al. (1998). "Fiber-Optic Nitric Oxide-Selective Biosensors and Nanosensors." Analytical Chemistry **70**(5): 971-976.

34. Reuel, N. F. and M. S. Strano (2014). Sensor for detecting analytes, Google Patents.

35. Scientific, T. f. (2010). Overview of affinity purification. Thermo Scientific Pierce Protein Purification Technical Handbook, Life technologies. **2:** 80.

36. Urh, M., et al. (2009). "Affinity chromatography: general methods." Methods Enzymol **463**: 417-438.

37. Cheung, R., et al. (2012). "Immobilized metal ion affinity chromatography: a review on its applications." Applied Microbiology & Biotechnology **96**(6): 1411-1420.

38. Schmuhl, R., et al. (2004). "Adsorption of Cu (II) and Cr (VI) ions by chitosan: Kinetics and equilibrium studies." Water Sa **27**(1): 1-8.

39. Sigal, G. B., et al. (1996). "A Self-Assembled Monolayer for the Binding and Study of Histidine-Tagged Proteins by Surface Plasmon Resonance." Analytical Chemistry **68**(3): 490-497

40. Lutang Wang, N. F. a. Z. H. (2012). Polyimide-Coated Fiber Bragg Grating Sensors for Humidity Measurements, intech

41. Li, Y., et al. (2014). "Multimode interference refractive index sensor based on coreless fiber." Photonic Sensors **4**(1): 21-27.

42. Liu, Z.-b., et al. (2014). "Refractive index sensing characterization of a singlemode–claddingless–singlemode fiber structure based fiber ring cavity laser." Optics Express **22**(5): 5037-5042.

43. Millipore - "Lab Water Tutorial, Water Contaminants and Water Monitoring". http://www.millipore.com/lab_water/clw4/tutorial&tabno=4, accessed 2011-08-15

44. Poole, I, " Fibre optic splicing. " from http://www.radioelectronics.com/info/telecommunications_networks/fiber-fibre-optics/optics-optical-splice-splicing.php.

45. Sulkowski, E. (1989). "The saga of IMAC and MIT." Bioessays **10**(5): 170-175.

46. Ueda, E. K. M., et al. (2003). "Current and prospective applications of metal ion–protein binding." Journal of Chromatography A **988**(1): 1-23.

47. Glusker, J. P. (1991). "Structural aspects of metal liganding to functional groups in proteins." Adv Protein Chem **42**: 1-76.

48. Rulíšek, L. r. and J. Vondrášek (1998). "Coordination geometries of selected transition metal ions (Co 2+, Ni 2+, Cu 2+, Zn 2+, Cd 2+, and Hg 2+) in metalloproteins." Journal of inorganic biochemistry **71**(3): 115-127

49. Prasanna, R. R. and M. A. Vijayalakshmi (2010). "Immobilized metal-ion affinity systems for recovery and structure–function studies of proteins at molecular, supramolecular, and cellular levels." Pure and Applied Chemistry **82**(1): 39-55.

50. Bornhorst, J. A. and J. J. Falke (2000). "Purification of Proteins Using Polyhistidine Affinity Tags." Methods in enzymology **326**: 245-254.

51. Firer, M. A. (2001). "Efficient elution of functional proteins in affinity chromatography." J Biochem Biophys Methods **49**(1-3): 433-442.

.